Supersolid Phase of Hard-Core Bosons on a Triangular Lattice

Massimo Boninsegni[1] and Nikolay Prokof'ev[2,3]
[1]Department of Physics, University of Alberta, Edmonton, Alberta T6G 2J1, Canada
[2]Department of Physics, University of Massachusetts, Amherst, Massachusetts 01003, USA
[3]Russian Research Center "Kurchatov Institute", 123182 Moscow, Russia
(Received 26 July 2005; published 28 November 2005)

We study properties of the supersolid phase observed for hard-core bosons on the triangular lattice near half-integer filling factor, and the phase diagram of the system at finite temperature. We find that the solid order is always of the $(2m, -m', -m')$ with m changing discontinuously from positive to negative values at half filling, in contrast with phases observed for Ising spins in a transverse magnetic field. At finite temperature we find two intersecting second-order transition lines: one in the 3-state Potts universality class and the other of the Kosterlitz-Thouless type.

DOI: 10.1103/PhysRevLett.95.237204 PACS numbers: 75.10.Jm, 05.30.Jp, 67.40.Kh, 74.25.Dw

Since the supersolid state of matter was introduced to physics nearly half a century ago and its theoretical feasibility was demonstrated [1], there has been a long history of experimental attempts to find it in nature [mostly in ^{4}He, see, e.g., Ref. [2]] along with numerical simulations and theoretical predictions for models of interacting lattice bosons. Recent years have seen a renewed interest in this topic. On the one hand, lattice bosons are no longer in the realm of idealized models and can be now studied in controlled experiments with ultracold atoms in optical potentials [3]. On the other hand, the nonclassical moment of inertia observed for solid ^{4}He samples in the torsional oscillator experiments by Kim and Chan [4] remains largely a mystery.

Hard-core bosons on triangular lattice with nearest-neighbor repulsion $V > 0$ and hopping $t > 0$ represent one of the simplest (and thus most promising from the experimental point of view) models displaying a supersolid phase in an extended region of the phase diagram. The model Hamiltonian is given by:

$$H = -t\sum_{\langle ij\rangle}(\hat{b}_i^\dagger \hat{b}_j + \text{H.c}) + V\sum_{\langle ij\rangle}\hat{n}_i\hat{n}_j - \mu\sum_i \hat{n}_i. \quad (1)$$

Here $\hat{b}_i^\dagger$ is the bosonic creation operator, $\hat{n}_i = \hat{b}_i^\dagger \hat{b}_i$, and μ is the chemical potential. A triangular lattice of $N = L \times L$ sites, with periodic boundary conditions, is assumed. The alternative formulation of (1) in terms of quantum spin-1/2 variables $\hat{s}_i$, namely,

$$H = -2t\sum_{\langle ij\rangle}(\hat{s}_i^x\hat{s}_j^x + \hat{s}_i^y\hat{s}_j^y) + V\sum_{\langle ij\rangle}\hat{s}_i^z\hat{s}_j^z - (\mu - 3V)\sum_i \hat{s}_i^z \quad (2)$$

provides a useful mapping to the XXZ magnet. The superfluid state of Eq. (1) for $t \gg V$ corresponds to the XY-ferromagnetic state of Eq. (2), while the solid state of bosons is equivalent to magnetic order in the $\hat{z}$ direction. At half-integer filling factor, $n(\mu = 3V) = 1/2$, the model has an exact particle-hole symmetry.

A robust confirmation of early mean-field predictions of a supersolid phase in the ground state of (1) [5] was obtained by means of Green function Monte Carlo (GFMC) simulations [6]. The supersolid phases identified in that study for densities away from half filling (i.e., for $\mu/V > 3$ and $\mu/V < 3$) can be viewed as solids, with filling factors $\nu = 2/3$ and $\nu = 1/3$, doped with holes and particles, respectively. In what follows, we denote them as supersolids $\mathcal{A}$ and $\mathcal{B}$. Density correlations in $\mathcal{A}$ and $\mathcal{B}$ have $\sqrt{3} \times \sqrt{3}$ ordering with the wave vector $\mathbf{Q} = (4\pi/3, 0)$. In $\mathcal{A}$ and $\mathcal{B}$ the average occupation numbers on three consecutive sites along any of the principal axes follow the sequence $(-2m, m', m')$ and $(2m, -m', -m')$, respectively (it is conventional to count densities from 1/2 to make connection with the magnetization in the spin language, $m_i = n_i - 1/2$); see Fig. 1.

The model (1) has been investigated in a series of recent papers, making use of advanced numerical techniques [7–9]. The proposed zero-temperature phase diagram is similar to that of Ref. [6], with the notable addition of a quantum superfluid-supersolid phase transition at $n = 1/2$ and $t/V \approx 0.115$ and the stable supersolid state persisting for smaller values of t/V. In Ref. [6] the system was thought to remain a disordered superfluid for arbitrary t/V. The discrepancy can be attributed to known limitations of the GFMC method [10].

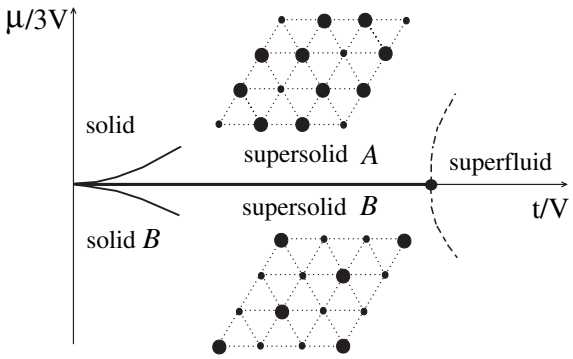

FIG. 1. Schematic phase diagram of Eq. (1) near half-integer filling factor.

Based on field-theoretic, exact diagonalization, and other arguments, Ref. [8] hints at the possibility of the $(m, 0, -m)$ density order in the ground state at $n = 1/2$ (state $\mathcal{C}$). These considerations involved, in particular, an analogy between the properties of Eq. (2), and those of the Ising antiferromagnet on the triangular lattice, in the presence of a transverse magnetic field [11]. If true, there should exist quantum $\mathcal{A} - \mathcal{C}$ and $\mathcal{C} - \mathcal{B}$ phase transitions away from half filling and three finite-temperature transitions of the Kosterlitz-Thouless (KT) type. Though Ref. [7] finds that the ground state is of the $\mathcal{A}$ or $\mathcal{B}$ type, it makes similar predictions for the finite-temperature phase diagram at $n = 1/2$ which follow from the assumption that spontaneous symmetry breaking between $\mathcal{A}$, $\mathcal{B}$, and their lattice translations is described by the six-clock model [12].

In what follows, we provide strong evidence that the supersolid state at half filling is always of either the $\mathcal{A}$ or $\mathcal{B}$ type. Our data suggest that there is a discontinuous transition from $\mathcal{A}$ to $\mathcal{B}$ at $\mu = 3V$ similar to the I-order phase transition (driven by the large energy of the $\mathcal{A} - \mathcal{B}$ domain walls). What makes it special is the exact particle-hole symmetry; structure factor, superfluid density, and energy remain continuous functions of μ through the transition line. For the supersolid $\mathcal{A}$ (or $\mathcal{B}$) with the threefold degenerate ground state, one expects to see the normal-superfluid KT and the solid-liquid 3-state Potts transitions, as temperature is increased. Moreover, the KT and Potts transitions are independent of each other and for $n \neq 1/2$ intersect on the phase diagram. The failure of the mean-field description and analogies with the transverse-field Ising model to predict the supersolid structure at $n = 1/2$ can be traced back to the U(1) symmetry of Eqs. (1) and (2), as noticed in [7]. For example, the $(1, 0, -1)$ state *cannot* be the true ground state at finite t in the limit of $t/V \to 0$ simply because it does not respect the particle conservation law.

We use the worm-algorithm Monte Carlo scheme in the lattice path-integral representation [13] to simulate Eq. (1). Since the structure factor

$$S(\mathbf{Q}) = \left\langle \left| \sum_{k=1}^{N} \hat{n}_k e^{i\mathbf{Q}\mathbf{r}_k} \right|^2 \right\rangle / N^2 \tag{3}$$

does not distinguish between supersolids $\mathcal{A}$, B, C we adopt the following strategy: for each system configuration, we compute the distribution of time-averaged occupation numbers, $\bar{n}_k = \beta^{-1} \int_0^\beta d\tau \hat{n}_k(\tau)$, and use it to determine the fraction of sites with $\bar{n}_k > 1/2$

$$n^+ = N^{-1} \sum_{k=1}^{N} \theta(\bar{n}_k - 1/2), \tag{4}$$

where $\theta(x)$ is the Heaviside function. $\mathcal{A}$, B, C density structures correspond to $n_A^+ = 2/3$, $n_C^+ = 0$, and $n_B^+ = 1/3$. Finite systems are characterized by broad probability distributions $P(n^+)$, and the formation of different solid orders can be seen as the development of sharp peaks, as the thermodynamic limit is approached.

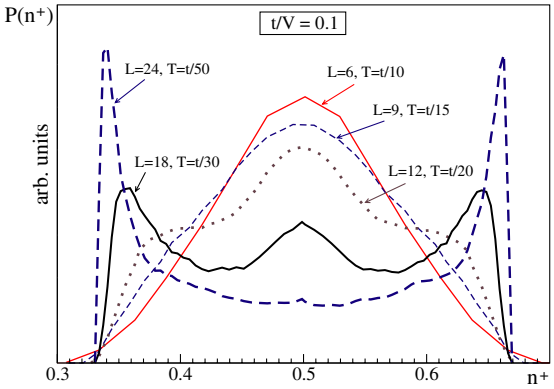

FIG. 2 (color online). Probability distributions $P(n^+)$ for different system sizes and temperatures at $\mu/V = 3$ and $t/V = 0.1$.

In Fig. 2 we show the evolution of the $P(n^+)$ distribution for the half-filled system at $V/t = 10$, i.e., close to the superfluid-supersolid transition point, estimated [7–9] at $V/t \approx 8.5$. The distribution is peaked at $n^+ = 0$ in the smallest system considered ($L = 6$), but, as the system size is increased, the weight is shifted toward the wings of the distribution. For $L = 18$, there are already three peaks with comparable height. Finally, in the $L = 24$ system we observe only two peaks corresponding to the supersolid phases $\mathcal{A}$ and $\mathcal{B}$. Though the probability density between the peaks is still measurable, the dynamics of the algorithm becomes very slow; it typically takes millions of Monte Carlo sweeps in order for the system to make a transition from the $\mathcal{A}$ to the $\mathcal{B}$ structure and vice versa. We have explicitly verified that configurations with $n^+ \approx 2/3$ and $n^+ \approx 1/3$ have density orders depicted as in Fig. 1, with a large contrast in density between sublattices. We have also checked that the $V/t = 10$, $L = 48$, $T = t/50$ system spontaneously develops either $\mathcal{A}$ or $\mathcal{B}$ order, starting from the initial configuration corresponding to the superfluid phase at $V/t = 5$.

In Fig. 3 we show what happens at larger values of V/t. Now, the central peak is already absent in relatively small $L = 12$ and $L = 18$ systems. We thus conclude that the nature of the supersolid state at half-integer filling factor is determined by the $\mathcal{A}$ and $\mathcal{B}$ structures, for *all* values of t/V for which a supersolid phase exists.

If spontaneous symmetry breaking of the ground state degeneracies is described by the six-clock model [12], one should observe three finite-temperature transitions for systems near half filling, and a solid phase with algebraic correlations "sandwiched" between the solid and normal liquid phases. This prediction was made in Ref. [7] for $n = 1/2$. Since the ground state was found here to be only of the $\mathcal{A}$ or $\mathcal{B}$ type, and we do not see why domain wall energies between translated $\mathcal{A}$ states are the same as between $\mathcal{A}$ and $\mathcal{B}$ states [in fact, the Landau theory prediction [7,8,14]

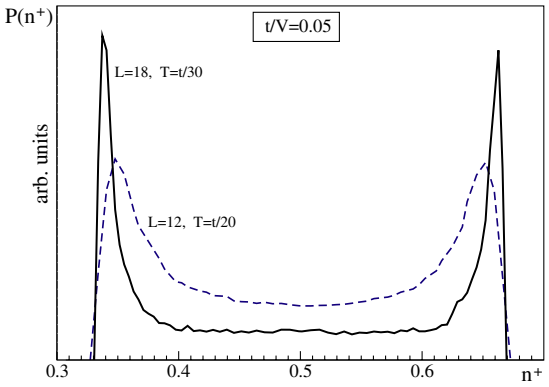

FIG. 3 (color online). Probability distributions $P(n^+)$ for different system sizes and temperatures at $\mu/V = 3$ and $t/V = 0.05$.

is that $\mathcal{A}$ and $\mathcal{B}$ states phase separate and have different average densities even at $\mu = 3V$], the finite-temperature phase diagram should instead feature the normal-superfluid KT and the liquid-solid 3-state Potts (for $n \neq 1/2$) transitions breaking U(1) and translation symmetry, respectively. At $n = 1/2$ we expect only one liquid-solid transition. An interesting question is whether transition lines simply intersect, or there are bicritical and tricritical points and I-order lines as observed for the similar model on the square lattice [15]. We performed simulations for two representative cases, one for constant chemical potential $\mu/V = 2.74$ (or density $n \approx 0.44$), and the other for constant $t/V = 0.1$.

In Fig. 4 we show typical data for the KT transition between the solid and supersolid phases. The transition is smeared by logarithmic finite-size effects, but the critical temperature can be still determined with good accuracy by

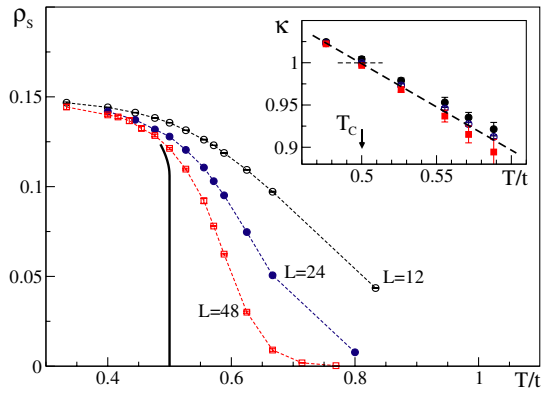

FIG. 4 (color online). Superfluid density in the vicinity of the KT transition for $t/V = 0.1$ and $\mu/V = 2.74$. The solid line is the thermodynamic curve calculated using Eq. (6) with $\kappa(T)$ deduced from the plot shown in the inset. Inset: solutions of Eq. (5) for different pairs of system sizes: $L_2 = 24$, $L_1 = 12$ (filled circles), $L_2 = 48$, $L_1 = 12$ (open circles), $L_2 = 48$, $L_1 = 24$ (filled squares). The dashed line is the linear fit $\kappa = 1 + 1.03(T_c - T)/t$ with $T_c/t = 0.50$.

utilizing the well-known renormalization flow and the universal jump of the superfluid density, ρ_s, at T_c. The data analysis is as follows [16]: we define $R = \pi\rho_s/2mT$ (where $m = 1/3t$ is the effective mass for the triangular lattice) and study the finite-size scaling of the data using KT renormalization group equations in the integral form

$$4\ln(L_2/L_1) = \int_{R_2}^{R_1} \frac{dt}{t^2(\ln(t) - \kappa) + t}. \tag{5}$$

The microscopic (system size independent) parameter κ is an analytic function of temperature, and the critical point corresponds to $R = 1$ at $\kappa = 1$. For $T < T_c$, the thermodynamic curve is defined by the equation

$$1/R + \ln R = \kappa(T), \tag{6}$$

with $\kappa = 1 + \kappa'(T_c - T)$. We use different pairs of system sizes in Eq. (5) to determine the $\kappa(T)$ curve, and obtain the location of the critical point from $\kappa(T_c) = 1$. The results are shown in the inset of Fig. 4. Data collapse and smooth analytic behavior of $\kappa(T)$ proves that the transition is indeed of the KT type. We used the same protocol and system sizes to determine other critical points.

In Fig. 5, we present our data for the transition into the state with the long-range density order. For the threefold degenerate $\mathcal{B}$ structure this transition is expected to be in the 3-state Potts universality class. The critical exponents are known exactly [17]: $\nu = 5/6$ and $\beta = 1/9$. We thus perform the data collapse using $L^{2\beta}S_{\mathbf{Q}} = f(\delta L^{1/\nu})$ where $\delta = (T - T_c)/t$ and T_c is the only fitting parameter. The result is shown in the inset of Fig. 5. This confirms the above-mentioned expectation, and establishes that there is only one transition to the solid phase (there are no visible finite-size effects below T_c).

Finally, we compute the phase diagram in the $(T/t, t/V)$ (at constant $\mu/V = 2.74$) and $(T/t, \mu/V)$ (at constant $t/V = 0.1$) planes and observe that KT and Potts transition lines form a simple cross for $n \neq 1/2$; i.e., the correspond-

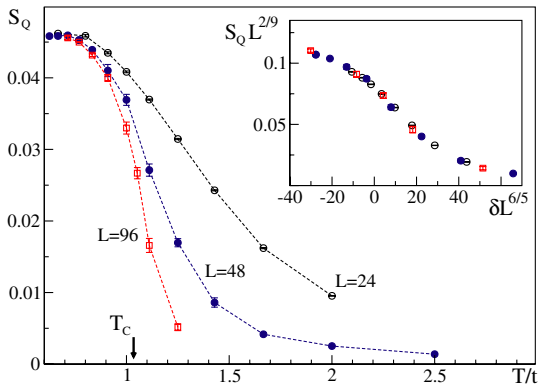

FIG. 5 (color online). Structure factor in the vicinity of the 3-state Potts transition for $t/V = 0.1$ and $\mu/V = 2.74$. Inset: data collapse using exact critical exponents for the 3-state Potts model [17] and $\delta = (T - T_c)/t$ with $T_c/t = 1.035$.

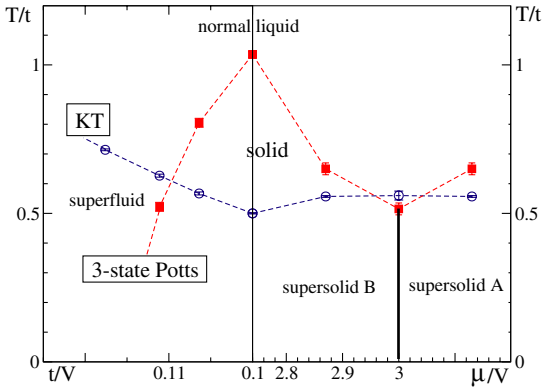

FIG. 6 (color online). Finite-temperature phase diagram for two representative cuts: the left panel is for fixed $\mu/V = 2.74$; the right panel is for fixed $t/V = 0.1$. The solid line indicates a degenerate I-order transition line between supersolids $\mathcal{B}$ and $\mathcal{A}$.

ing order parameter fields are not strongly interacting, see Fig. 6. The transition temperature to the superfluid and supersolid states in this part of the phase diagram is determined by the hopping amplitude. Within the statistical uncertainties of our calculation, KT and Potts transition temperatures cannot be distinguished at $\mu/V = 3$.

We did not see evidence for the algebraic solid state at $\mu = 3V$. The finite-size scaling for the supersolid-solid transition at $\mu = 3V$ is consistent with the 3-state Potts universality, though the data collapse is not as impressive as in Fig. 4 (the other alternative is the KT transition).

It is instructive to understand why the $(m, 0, -m)$ phase for the Hamiltonian (1) is not an obvious ground state. At the mean-field level, $\mathcal{C}$ has a better energy than $\mathcal{A}$ or $\mathcal{B}$. For the transverse-field Ising model [11] the $(1, 0, -1)$ spin arrangement is obtained by orienting the middle spin along the magnetic field direction, i.e., putting it in the equal-amplitude superposition of up and down states. In bosonic language, it corresponds to the superposition of states with one or zero particles on a given site. Such a state can not be reconciled with the Hamiltonian (1) which conserves the particle number. Any noninteger average occupation number necessarily involves hopping transitions to the nearest-neighbor sites. In the $(1, 0, -1)$ structure the middle site is completely surrounded by the fully occupied or empty sites and thus cannot be the ground state of the system even in the limit of $t/V \to \infty$. The problem appears to be inherently quantum with no obvious solution at the mean-field level.

We are grateful M. Troyer, A. Paramekanti, K. Damle, and A. Burkov for stimulating discussions. The research was supported by the National Science Foundation under Grant No. PHY-0426881, by the Petroleum Research Fund of the American Chemical Society under research Grant No. 36658-AC5, and by the Natural Science and Engineering Research Council of Canada under research Grant No. G121210893.

[1] O. Penrose and L. Onsager, Phys. Rev. **104**, 576 (1956); A. F. Andreev and I. M. Lifshitz, Sov. Phys. JETP **29**, 1107 (1960); G. Chester, Phys. Rev. A **2**, 256 (1970); A. J. Leggett, Phys. Rev. Lett. **25**, 1543 (1970).
[2] M. W. Meisel, Physica (Amsterdam) **B178**, 121 (1992).
[3] M. Greiner, C. A. Regal, and D. S. Jin, Nature (London) **415**, 39 (2002).
[4] E. Kim and M. H. W. Chan, Nature (London) **427**, 225 (2004); Science **305**, 1941 (2004).
[5] G. Murthy, D. Arovas, and A. Auerbach, Phys. Rev. B **55**, 3104 (1997).
[6] M. Boninsegni, J. Low Temp. Phys. **132**, 39 (2003).
[7] D. Heidarian and K. Damle, Phys. Rev. Lett. **95**, 127206 (2005).
[8] R. G. Melko, A. Paramekanti, A. A. Burkov, A. Vishwanath, D. N. Sheng, and L. Balents, Phys. Rev. Lett. **95**, 127207 (2005).
[9] S. Wessel and M. Troyer, Phys. Rev. Lett. **95**, 127205 (2005).
[10] Working with a finite population of random walkers in the GFMC method has the effect of biasing estimates for the static structure factor, required to establish the presence of diagonal long-range order. Such a bias can in principle be eliminated by increasing the size of the population, but this is often impractical. See, for instance, M. Calandra Bonaura and S. Sorella, Phys. Rev. B **57**, 11 446 (1998).
[11] R. Moessner and S. L. Sondhi, Phys. Rev. B **63**, 224401 (2001); R. Moessner, S. L. Sondhi, and P. Chandra, Phys. Rev. B **64**, 144416 (2001); S. V. Isakov and R. Moessner, Phys. Rev. B **68**, 104409 (2003).
[12] J. Jose, L. Kadanoff, S. Kirkpatrick, and D. Nelson, Phys. Rev. B **16**, 1217 (1977).
[13] N. V. Prokof'ev, B. V. Svistunov, and I. S. Tupitsyn, Phys. Lett. **238**, 253 (1998); Sov. Phys. JETP **87**, 310 (1998).
[14] A. A. Burkov and L. Balents, Phys. Rev. B **72**, 134502 (2005).
[15] G. G. Batrouni and R. T. Scalettar, Phys. Rev. Lett. **84**, 1599 (2000); F. Hébert, G. G. Batrouni, R. T. Scalettar, G. Schmid, M. Troyer, and A. Dorneich, Phys. Rev. B **65**, 014513 (2002); G. Schmid, S. Todo, M. Troyer, and A. Dorneich, Phys. Rev. Lett. **88**, 167208 (2002); K. Bernardet, G. G. Batrouni, J.-L. Meunier, G. Schmid, M. Troyer, and A. Dorneich, Phys. Rev. B **65**, 104519 (2002).
[16] N. Prokof'ev and B. Svistunov, Phys. Rev. A **66**, 043608 (2002).
[17] S. Alexander, Phys. Lett. **54A**, 353 (1975).